Acta Crystallographica Section F
Structural Biology Communications
ISSN 2053-230X

Crystallization and preliminary X-ray diffraction analysis of the interleukin-3 alpha receptor bound to the Fab fragment of antibody CSL362

Sophie E. Broughton,[a] Timothy R. Hercus,[b] Tracy L. Nero,[a] Urmi Dhagat,[a]* Catherine M. Owczarek,[c] Matthew P. Hardy,[c] Louis J. Fabri,[c] Pierre D. Scotney,[c] Andrew D. Nash,[c] Nicholas J. Wilson,[c] Angel F. Lopez[b] and Michael W. Parker[a,d]

[a]Australian Cancer Research Foundation Rational Drug Discovery Centre and Biota Structural Biology Laboratory, St Vincent's Institute of Medical Research, Fitzroy, Victoria, Australia, [b]Division of Human Immunology, The Centre for Cancer Biology, SA Pathology, Adelaide, South Australia, Australia, [c]CSL Limited, Bio21 Molecular Science and Biotechnology Institute, University of Melbourne, Parkville, Victoria, Australia, and [d]Department of Biochemistry and Molecular Biology, Bio21 Molecular Science and Biotechnology Institute, University of Melbourne, Parkville, Victoria, Australia

Correspondence e-mail: udhagat@svi.edu.au

Received 23 December 2013
Accepted 4 February 2014

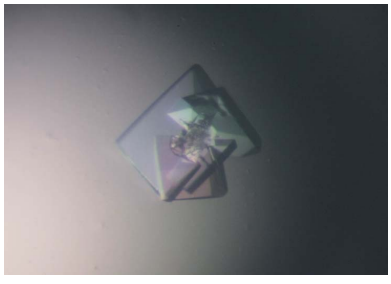

© 2014 International Union of Crystallography
All rights reserved

Interleukin-3 (IL-3) is a member of the beta common family of cytokines that regulate multiple functions of myeloid cells. The IL-3 receptor-specific alpha subunit (IL3Rα) is overexpressed on stem cells/progenitor cells of patients with acute myeloid leukaemia, where elevated receptor expression correlates clinically with a reduced patient survival rate. The monoclonal antibody (MAb) CSL362 is a humanized MAb derived from the murine MAb 7G3, originally identified for its ability to specifically recognize the human IL-3 receptor and for blocking the signalling of IL-3 in myeloid and endothelial cells. In order to elucidate the molecular mechanism of CSL362 antagonism, a preliminary structure of human IL3Rα in complex with the MAb CSL362 has been determined.

1. Introduction

IL-3, IL-5 and GM-CSF belong to a family of cytokines that regulate the function of haematopoietic cells. The receptor for IL-3 is expressed on haematopoietic cells and comprises an alpha chain (IL3Rα) and a beta common subunit (βc) that is shared with the receptors for IL-5 and GM-CSF. IL3Rα binds cytokine with low affinity (K_d = 100 nM), but the presence of βc converts this to high-affinity binding (K_d = 100 pM) and causes receptor heterodimerization and activation of signal transduction pathways (Stomski *et al.*, 1996). Downstream signalling is initiated *via* the phosphorylation of βc receptor-associated JAK2, which results in transphosphorylation of tyrosine residues in βc and signalling through the JAK/STAT, Ras-MAP kinase and PI3-kinase pathways (Guthridge *et al.*, 1998).

IL-3 activity appears to be pathogenically linked to leukaemia, in that autocrine- or paracrine-produced IL-3 (Jiang *et al.*, 1999) can act as a growth factor for acute and chronic myeloid leukaemia (AML and CML). Furthermore, AML and CML progenitor/stem cells overexpress IL3Rα, presumably conferring them with a survival and proliferative advantage (Jordan *et al.*, 2000; Testa *et al.*, 2002; Jin *et al.*, 2009). We have previously developed the murine monoclonal antibody (MAb) 7G3 that specifically recognizes human IL3Rα and blocks the signalling of IL-3 in leukaemia cells, basophils and endothelial cells (Sun *et al.*, 1996). It was subsequently shown to eliminate AML stem cells in a mouse model of human AML (Jin *et al.*, 2009) by a mechanism involving IL-3 antagonism and NK cell-mediated immune effector function. Since MAb 7G3 is able to target the IL3Rα receptor that is overexpressed on leukaemic cells, it offered a therapeutic opportunity. 7G3 was subsequently humanized and optimized for antibody-dependent cytotoxicity against leukaemic cells and termed CSL362 (Nievergall *et al.*, 2013). Based on this activity, CSL362 has recently entered clinical trials for the treatment of patients with AML (http://ClinicalTrials.gov identifier NCT01632852). As part of our studies to elucidate the molecular basis of IL-3 receptor antagonism, we have obtained crystals of human IL3Rα in complex with CSL362.

2. Experimental procedures and results

2.1. Expression and purification of soluble IL3Rα subunit

A DNA fragment encoding the native signal peptide sequence and the complete extracellular domain of IL3Rα (sIL3Rα) from Lys20

through to Ser306 (Fig. 1*a*) and including the Lys144 splice variant was cloned into the pFastBac1 vector (Invitrogen). The resulting pFastBac1:sIL3Rα plasmid was transformed into DH10Bac *Escherichia coli*, from which recombinant bacmid DNA was isolated and transfected into Sf9 insect cells using the Cellfectin reagent (Invitrogen). Following three rounds of recombinant virus propagation, large-scale expression of sIL3Rα was performed by infection of Sf9 cells grown in Sf-900 II serum-free medium (Life Technologies). The supernatant was harvested following incubation after 5 d, and sIL3Rα was immunoaffinity-purified using the IL3Rα-specific MAb 9F5 (Sun *et al.*, 1996) coupled to HiTrap NHS-activated HP columns (GE Healthcare). Bound protein was eluted using 500 m*M* NaCl, 50 m*M* phosphoric acid pH 2.4 and immediately neutralized by collection in tubes containing a 4% final volume of 2 *M* Trizma base. Affinity-purified sIL3Rα was further purified by size-exclusion chromatography (SEC) using a Superdex 200 column (26 × 600 mm, GE Healthcare) operated at 2 ml min^{-1} at 4°C with a running buffer consisting of 150 m*M* NaCl, 50 m*M* sodium phosphate pH 7.0. The yield of purified sIL3Rα was typically 0.15–0.3 mg per litre of supernatant.

2.2. Generation and purification of the IL3Rα–CSL362 binary complex

The recombinant Fab fragment of CSL362 was generated by cloning the entire kappa light chain and a truncated heavy chain (Fig. 1*b*), where a stop codon was introduced after amino acid 247, separately into pcDNA3.1 (Invitrogen, Life Technologies). Transient transfections (1 l) of expression plasmids encoding the CSL362 Fab fragment were performed using the 293fectin transfection reagent (Invitrogen, Life Technologies) and FS293F cells according to the manufacturer's instructions in 3 l Fernbach flasks (Corning) for 6 d at 37°C in a shaking incubator (100 rev min^{-1}) with an atmosphere of 8% CO_2. Cultures were supplemented at 4 h post-transfection with Pluronic F68 (Gibco, Life Technologies) to a final concentration of 0.1%(*v*/*v*) and 24 h post-transfection with LucraTone Lupin (Millipore) to a final concentration of 0.5%(*v*/*v*). The cell culture supernatants were harvested by centrifugation at 2500 rev min^{-1} and were passed through a 0.45 µm filter (Nalgene) prior to purification. CSL362 Fab was purified by affinity chromatography with KappaSelect (GE Healthcare Life Sciences). The resin was equilibrated with 137 m*M* NaCl, 2.7 m*M* KCl, 10 m*M* sodium phosphate pH 7.3 and the bound protein was step-eluted with 0.1 *M* glycine pH 3.0 into a 1/10 volume of 3 *M* Tris–HCl pH 8.3. The affinity-purified Fab was buffer-exchanged into 10 m*M* HEPES pH 7.4 using a HiPrep 26/10 Desalting column (GE Healthcare Life Sciences) packed with Sephadex G-25 Fine resin. The CSL362 Fab was concentrated to 12 mg ml^{-1} using an Amicon Ultracel 10K (Millipore). The IL3Rα–CSL362 complex was prepared by incubating 4.5 mg of sIL3Rα with a 1.5 molar excess of CSL362 Fab at 25°C for 1 h and then fractionating the mixture by SEC as described above. Peak fractions were analyzed by SDS–PAGE for the presence of the individual protein components.

Soluble IL3Rα subunit

```
KEDPNPPITNLRMKAKAQQLTWDLNRNVTDIECVKDADYSMPAVNNSYCQFGAISLCEVT     79

NYTVRVANPPFSTWILFPENSGKPWAGAENLTCWIHDVDFLSCSWAVGPGAPADVQYDLY    139

LNVAKRQQYECLHYKTDAQGTRIGCRFDDISRLSSGSQSSHILVRGRSAAFGIPCTDKFV    199

VFSQIEILTPPNMTAKCNKTHSFMHWKMRSHFNRKFRYELQIQKRMQPVITEQVRDRTSF    259

QLLNPGTYTVQIRARERVYEFLSAWSTPQRFECDQEEGVNTRAWRTS                 306
```

(*a*)

CSL362 Heavy Chain Fab fragment

```
EVQLVQSGAEVKKPGESLKISCKGSGYSFTDYYMKWARQMPGKGLEWMGDIIPSNGATFY     60
                              CDR1                    CDR2
NQKFKGQVTISADKSISTTYLQWSSLKASDTAMYYCARSHLLRASWFAYWGQGTMVTVSS    120
                                        CDR3
ASTKGPSVFPLAPSSKSTSGGTAALGCLVKDYFPEPVTVSWNSGALTSGVHTFPAVLQSS    180
Linker
GLYSLSSVVTVPSSSLGTQTYICNVNHKPSNTKVDKKVEPKSCDKTHT               228
```

CSL362 Light Chain Fab fragment

```
DIVMTQSPDSLAVSLGERATINCESSQSLLNSGNQKNYLTWYQQKPGQPPKPLIYWASTR     60
                          CDR1                          CDR2
ESGVPDRFSGSGSGTDFTLTISSLQAEDVAVYYCQNDYSYPYTFGQGTKLEIKRTVAAPS    120
                                   CDR3                Linker
VFIFPPSDEQLKSGTASVVCLLNNFYPREAKVQWKVDNALQSGNSQESVTEQDSKDSTYS    180

LSSTLTLSKADYEKHKVYACEVTHQGLSSPVTKSFNRGEC                       220
```

(*b*)

Figure 1
Sequences of sIL3Rα and the CSL362 Fab heavy chain and light chain. (*a*) The sequence of IL3Rα showing the 287 residues. (*b*) The sequence of the CSL362 heavy chain Fab shows the complete 228 residues, including the variable domain residues 1–112, the linker region (dashed underline) and the constant domain residues 124–228. The sequence of the CSL362 light chain Fab shows the complete 220 residues, including the variable domain residues 1–111, the linker region (dashed underline) and the constant domain residues 118–220.

Table 1
Diffraction data statistics.

Values in parentheses are for the outermost resolution shell.

Space group	$P2_1$
Unit-cell parameters (Å, °)	a = 88.3, b = 120.7, c = 93.0, α = 90, β = 97.5, γ = 90
Wavelength (Å)	0.954
Resolution range (Å)	49.0–2.80 (2.90–2.80)
Total observations	140965
Unique reflections	46204 (4593)
Multiplicity	3.1 (3.1)
Completeness (%)	98.3 (98.2)
Mean $I/\sigma(I)$	28.7 (2.9)
$R_{\rm merge}$†	0.064 (0.54)
$R_{\rm p.i.m.}$	0.078 (0.65)
$R_{\rm r.i.m.}$	0.043 (0.35)

† $R_{\rm merge} = \sum_{hkl}\sum_i |I_i(hkl) - \langle I(hkl)\rangle| / \sum_{hkl}\sum_i I_i(hkl)$, where $I_i(hkl)$ is the intensity of the ith measurement of a symmetry-related reflection with indices hkl.

2.3. Protein crystallization

Crystallization trials of the IL3Rα–CSL362 complex were set up using the PACT protein crystallization screen (Newman *et al.*, 2005) with the protein at a concentration of 20 mg ml^{-1}. Crystallization was performed in-house using the hanging-drop vapour-diffusion method at 22°C. 1 µl each of protein and precipitant solutions was mixed together and equilibrated over 1 ml reservoir solution. Tetragonally shaped crystals appeared after 3 d in 20% PEG 3350, 200 m*M* sodium malonate, 100 m*M* bis-tris propane chloride pH 6.5. After screening around the original crystal condition, the best crystals were obtained in 22% PEG 3350, 200 m*M* sodium malonate, 100 m*M* citrate buffer pH 6.2–6.5 with maximal dimensions of 0.45 × 0.2 × 0.1 mm (Fig. 2).

2.4. Data collection and preliminary X-ray analysis

For data collection, all crystals were dipped quickly and consecutively into 5, 10 and 15%(*v*/*v*) ethylene glycol in crystallization buffer. Data were collected on the MX2 beamline at the Australian Synchrotron, Clayton, Victoria. Data collection was controlled using the *Blu-Ice* software (McPhillips *et al.*, 2002) and data were processed with the *HKL*-2000 suite (Otwinowski & Minor, 1997). The crystals diffracted to a resolution of 2.8 Å (Fig. 3) in the monoclinic space group $P2_1$. The space group and unit-cell parameters were consistent with there being two complexes in the asymmetric unit, giving a Matthews coefficient (Matthews, 1968) of 3.12 Å^3 Da^{-1} and an estimated solvent content of 61%. Data-collection statistics are given in Table 1.

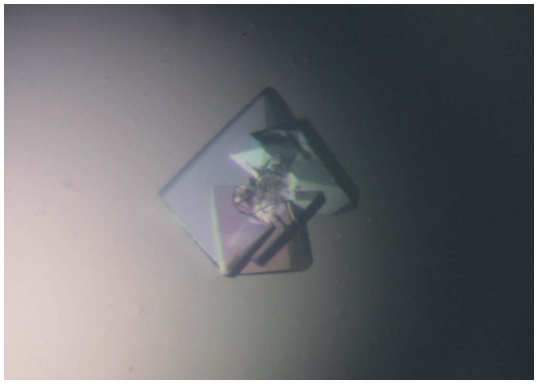

Figure 2
Crystals of IL3Rα–CSL362 grown by vapour diffusion at 22°C in a mother liquor consisting of 22% PEG 3350, 200 m*M* sodium malonate, 100 m*M* citrate buffer pH 6.4. The larger crystal in the centre of the picture is approximately 0.03 × 0.1 × 0.1 mm in size.

The structure was solved with the program *Phaser* (McCoy *et al.*, 2007) using a number of high-resolution input models for the heavy- and light-chain Fab fragments based on predicted secondary structure and sequence identity. The final models selected by *Phaser* were from the light chain of an antibody complex with nitric oxide reductase from *Pseudomonas aeruginosa* (PDB entry 3o0r; Hino *et al.*, 2010) and the heavy chain of a humanized apo Lt3015 anti-lysophosphatidic acid antibody Fab fragment (PDB entry 3qct; Fleming *et al.*, 2011; final TFZ of 24.5). The sequence identity between CSL362 and the heavy chain of 3o0r is 56% and between the two light chains it is 61%. The sequence identity between CSL362 and 3qct for the heavy and light chains is 83 and 82%, respectively.

A range of models were trialled for use as a search model for the IL3Rα component of the complex, including IL13Rα1 (PDB entry 3bpo; LaPorte *et al.*, 2008), IL13Rα2 (PDB entry 3lb6; Lupardus *et al.*, 2010), IL5Rα (PDB entries 3qt2 and 3va2; Patino *et al.*, 2011; Kusano *et al.*, 2012) and the partial GMRα structure from the ternary GM-CSF complex (PDB entry 3cxe; Hansen *et al.*, 2008). Aside from the partial GMRα structure all models included the fibronectin type III three-domain architecture [domains D2, D3 and N-terminal domain (NTD)]. As these search models resulted in suboptimal molecular-replacement solutions with poor translation-function *Z*-scores, the human IL3Rα extracellular domain sequence P26951.1 (amino acids 19–305) was used as the query sequence for *HHpred* (http://toolkit.tuebingen.mpg.de/hhpred; Söding, 2005). The sequence alignment of the closest IL3Rα homologues was created using the automatic mode within *HHpred*. The IL5Rα *A* chain (PDB entry 3qt2) was identified as the best structural template and the generated sequence alignment was then used to construct an IL3Rα homology model using the program *Modeller* v.9.9 (http://toolkit.tuebingen.mpg.de/modeller#; Sali *et al.*, 1995). The IL3Rα homology model was used as the final search model for molecular replacement without any geometry optimization.

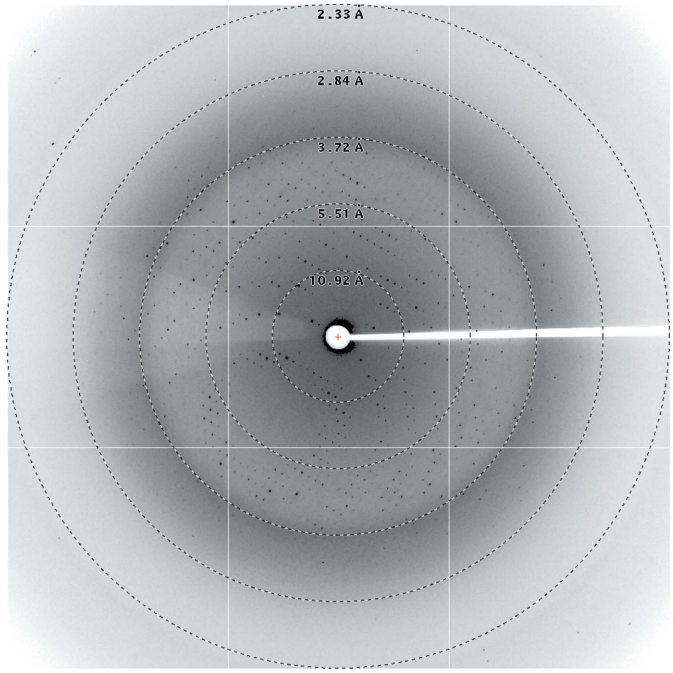

Figure 3
X-ray diffraction pattern from an IL3Rα–CSL362 crystal recorded at the Australian Synchrotron with 0.5° oscillations, showing visible diffraction to 2.8 Å resolution.

The final solution from *Phaser* had two IL3Rα–CSL362 complexes in the asymmetric unit with a translation-function *Z*-score of 27.7. Initially, only two CSL362 molecules and a single IL3Rα molecule were found *via* molecular replacement. The NTD of the second IL3Rα molecule was placed *via* symmetry operators; owing to the differing domain angles between the two complexes, D2 and D3 were then manually placed in the electron-density map using *Coot* (Emsley & Cowtan, 2004) followed by two subsequent rounds of rigid-body refinement using *REFMAC*5 (Murshudov *et al.*, 2011). The resulting refinement clearly indicates the presence of two non-identical IL3Rα–CSL362 complexes. Because of differences between IL3Rα and the homology model and the unique CDR loops in CSL362, significant rebuilding and refinement will be required to complete the structure. We anticipate that the final structure will reveal what IL3Rα looks like, the detailed epitope recognized by the antibody and the molecular basis for the antibody's antagonism of the receptor.

This research was partly undertaken on the MX2 beamline at the Australian Synchrotron, Victoria, Australia. We thank the beamline staff for their assistance. We acknowledge the technical assistance of Anna Sapa for help with protein production and Dr Mike Gorman for his crystallography advice. This work was supported by grants from the National Health and Medical Research Council of Australia (NHMRC) to TRH, MWP and AFL, from Cancer Australia to AFL and from the Australian Cancer Research Foundation to MWP. Funding from the Victorian Government Operational Infrastructure Support Scheme to St Vincent's Institute is acknowledged. UD and MWP are NHMRC Postdoctoral and Research Fellows, respectively, and SEB is a Postdoctoral Fellow supported by the Leukaemia Foundation.

References

Emsley, P. & Cowtan, K. (2004). *Acta Cryst.* D**60**, 2126–2132.
Fleming, J. K., Wojciak, J. M., Campbell, M. A. & Huxford, T. (2011). *J. Mol. Biol.* **408**, 462–476.
Guthridge, M. A., Stomski, F. C., Thomas, D., Woodcock, J. M., Bagley, C. J., Berndt, M. C. & Lopez, A. F. (1998). *Stem Cells*, **16**, 301–313.
Hansen, G., Hercus, T. R., McClure, B. J., Stomski, F. C., Dottore, M., Powell, J., Ramshaw, H., Woodcock, J. M., Xu, Y., Guthridge, M., McKinstry, W. J., Lopez, A. F. & Parker, M. W. (2008). *Cell*, **134**, 496–507.
Hino, T., Matsumoto, Y., Nagano, S., Sugimoto, H., Fukumori, Y., Murata, T., Iwata, S. & Shiro, Y. (2010). *Science*, **330**, 1666–1670.
Jiang, X., Lopez, A., Holyoake, T., Eaves, A. & Eaves, C. (1999). *Proc. Natl Acad. Sci. USA*, **96**, 12804–12809.
Jin, L., Lee, E. M., Ramshaw, H. S., Busfield, S. J., Peoppl, A. G., Wilkinson, L., Guthridge, M. A., Thomas, D., Barry, E. F., Boyd, A., Gearing, D. P., Vairo, G., Lopez, A. F., Dick, J. E. & Lock, R. B. (2009). *Cell Stem Cell*, **5**, 31–42.
Jordan, C. T., Upchurch, D., Szilvassy, S. J., Guzman, M. L., Howard, D. S., Pettigrew, A. L., Meyerrose, T., Rossi, R., Grimes, B., Rizzieri, D. A., Luger, S. M. & Phillips, G. L. (2000). *Leukemia*, **14**, 1777–1784.
Kusano, S., Kukimoto-Niino, M., Hino, N., Ohsawa, N., Ikutani, M., Takaki, S., Sakamoto, K., Hara-Yokoyama, M., Shirouzu, M., Takatsu, K. & Yokoyama, S. (2012). *Protein Sci.* **6**, 850–864.
LaPorte, S. L., Juo, Z. S., Vaclavikova, J., Colf, L. A., Qi, X., Heller, N. M., Keegan, A. D. & Garcia, K. C. (2008). *Cell*, **132**, 259–272.
Lupardus, P. J., Birnbaum, M. E. & Garcia, K. C. (2010). *Structure*, **18**, 332–342.
Matthews, B. W. (1968). *J. Mol. Biol.* **33**, 499–501.
McCoy, A. J., Grosse-Kunstleve, R. W., Adams, P. D., Winn, M. D., Storoni, L. C. & Read, R. J. (2007). *J. Appl. Cryst.* **40**, 658–674.
McPhillips, T. M., McPhillips, S. E., Chiu, H.-J., Cohen, A. E., Deacon, A. M., Ellis, P. J., Garman, E., Gonzalez, A., Sauter, N. K., Phizackerley, R. P., Soltis, S. M. & Kuhn, P. (2002). *J. Synchrotron Rad.* **9**, 401–406.
Murshudov, G. N., Skubák, P., Lebedev, A. A., Pannu, N. S., Steiner, R. A., Nicholls, R. A., Winn, M. D., Long, F. & Vagin, A. A. (2011). *Acta Cryst.* D**67**, 355–367.
Newman, J., Egan, D., Walter, T. S., Meged, R., Berry, I., Ben Jelloul, M., Sussman, J. L., Stuart, D. I. & Perrakis, A. (2005). *Acta Cryst.* D**61**, 1426–1431.
Nievergall, E., Ramshaw, H. S., Yong, A. S. M., Biondo, M., Busfield, S. J., Vairo, G., Lopez, A. F., Hughes, T. P., White, D. L. & Hiwase, D. K. (2013). *Blood*, doi:10.1182/blood-2012-12-475194.
Otwinowski, Z. & Minor, W. (1997). *Methods Enzymol.* **276**, 307–326.
Patino, E., Kotzsch, A., Saremba, S., Nickel, J., Schmitz, W., Sebald, W. & Mueller, T. D. (2011). *Structure*, **19**, 1864–1875.
Sali, A., Potterton, L., Yuan, F., van Vlijmen, H. & Karplus, M. (1995). *Proteins*, **23**, 318–326.
Söding, J. (2005). *Bioinformatics*, **21**, 951–960.
Stomski, F. C., Sun, Q., Bagley, C. J., Woodcock, J., Goodall, G., Andrews, R. K., Berndt, M. C. & Lopez, A. F. (1996). *Mol. Cell. Biol.* **16**, 3035–3046.
Sun, Q., Woodcock, J. M., Rapoport, A., Stomski, F. C., Korpelainen, E. I., Bagley, C. J., Goodall, G. J., Smith, W. B., Gamble, J. R., Vadas, M. A. & Lopez, A. F. (1996). *Blood*, **87**, 83–92.
Testa, U., Riccioni, R., Militi, S., Coccia, E., Stellacci, E., Samoggia, P., Latagliata, R., Mariani, G., Rossini, A., Battistini, A., Lo-Coco, F. & Peschle, C. (2002). *Blood*, **100**, 2980–2988.